2013 European Control Conference (ECC)
July 17-19, 2013, Zürich, Switzerland.

Fast and Saturating Attitude Control for a Quadrotor Helicopter

Oliver Fritsch, Bernd Henze and Boris Lohmann

***Abstract*— In this paper a continuous, nonlinear state feedback attitude controller for a quadrotor helicopter is presented. The design is based on an energy shaping approach and prioritizes the alignment of the thrust direction due to its prominent role for the translational dynamics. Since the controller tends to saturate the control torques, it achieves short settling times. Almost global asymptotic stability of the desired attitude is proven for arbitrary unknown moment of inertia matrices and the performance of the closed loop system is analyzed by simulations.**

I. INTRODUCTION

A quadrotor helicopter is a highly maneuverable vertical take-off and landing aircraft, which offers the ability of hovering. As shown in Fig. 1, it is basically a rigid body with four rotors arranged in a common plane which generate thrust forces and drag moments. The effects of the four single rotors can be summarized in the center of gravity as a total thrust force F perpendicular to the plane and a torque vector $\boldsymbol{\tau} = \begin{bmatrix}\tau_x & \tau_y & \tau_z\end{bmatrix}^T$. Since the direction of the (total) thrust is body-fixed, the execution of almost all translational motions requires tilting the whole quadrotor helicopter systematically. Consequently, a desired thrust direction is usually the output of a higher level position controller or the remote control command of a human operator and is forwarded to the attitude control. Accordingly, the thrust direction plays a prominent role in the attitude control task of a quadrotor and its alignment should be prioritized compared to the orientation around the thrust axis. This paper extends the thrust direction control presented in [5] to a complete attitude control which still focuses on the alignment of the thrust. An energy shaping approach is used to design a continuous state feedback controller for the nonlinear system. The resulting controller is able to exploit the available control torques to a great extent or even saturate them during the regulation process leading to a fast transient behavior. Almost global asymptotic stability of the desired attitude is proven for arbitrary unknown moment of inertia matrices.

Though our control task belongs to the broad field of rigid body attitude control (see e.g. [2] for a survey of the topic), only a few works consider control input constraints [6], [3], [8] and even less address thrust direction control or analogous problems [7], [3]. To the best knowledge of the authors a saturating attitude control prioritizing one body axis has not been presented before.

In Section II we give a brief introduction into attitude parametrization using quaternions. A detailed problem statement together with the plant model is introduced in Section III. Based on an energy shaping approach, the attitude controller is developed in Section IV, before almost global asymptotic stability of the desired attitude is proven in Section V. In Section VI the performance of the controller is studied in simulations before conclusions are drawn in Section VII, along with an outlook for future research.

O. Fritsch, B. Henze and B. Lohmann are with the Institute of Automatic Control, Technische Universität München (TUM), Germany oliver.fritsch@tum.de, lohmann@tum.de

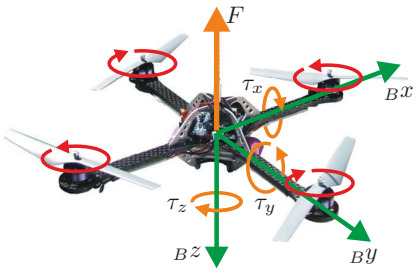

Fig. 1. Quadrotor with body-fixed frame B and control inputs $F, \tau_x, \tau_y, \tau_z$.

II. ATTITUDE PARAMETRIZATION

In order to specify the attitude of the quadrotor we use a body-fixed frame B attached to the aircraft as shown in Fig. 1 and an inertial *North East Down* reference frame N. The origins of both frames are located at the center of mass of the vehicle. In body coordinates, the thrust vector always points in the negative z-direction. It follows that aligning the thrust direction of the quadrotor helicopter is equivalent to aligning the z-axis of the body-fixed frame.

For the attitude parametrization we use quaternions (see e.g. [11]), which are directly built up by the axis and the angle information of a rotation. This parametrization admits an advantageous decomposition into two principal rotations which is a crucial step for the development of our control law. In more detail this decomposition can be found in [5] and in a slightly different context also in [4].

A. Interpretation of a quaternion

A unit quaternion $\mathbf{q} \in \mathcal{S}^3$ with $\mathcal{S}^3 = \{\mathbf{q} \in \mathbb{R}^4 : \mathbf{q}^T\mathbf{q} = 1\}$ can be used to describe the rotation that maps a coordinate frame X on a coordinate frame Y. Its four elements are composed of the angle and axis information of this rotation

$$\mathbf{q} = \begin{bmatrix} q_1 \\ q_2 \\ q_3 \\ q_4 \end{bmatrix} = \begin{bmatrix} \mathbf{e} \sin\dfrac{\alpha}{2} \\ \cos\dfrac{\alpha}{2} \end{bmatrix}, \tag{1}$$

where $\mathbf{e} \in \mathbb{R}^3$ is the normalized axis vector and α is the rotation angle. It is clear from (1) that $-\mathbf{q}$ represents the

same mapping from X to Y and that the reverse rotation from Y to X is given by the conjugate quaternion

$$\bar{\mathbf{q}} = \begin{bmatrix} -q_1 & -q_2 & -q_3 & q_4 \end{bmatrix}^T . \tag{2}$$

B. Multiplication of quaternions

The multiplication of two quaternions is defined as

$$\mathbf{r} = \mathbf{q} \circ \mathbf{p} = \underbrace{\begin{bmatrix} p_4 & p_3 & -p_2 & p_1 \\ -p_3 & p_4 & p_1 & p_2 \\ p_2 & -p_1 & p_4 & p_3 \\ -p_1 & -p_2 & -p_3 & p_4 \end{bmatrix}}_{\mathbf{W}(\mathbf{p})} \begin{bmatrix} q_1 \\ q_2 \\ q_3 \\ q_4 \end{bmatrix} \tag{3}$$

and corresponds to a consecutive execution of the rotations parametrized by $\mathbf{q}$ and $\mathbf{p}$. The second rotation defined by $\mathbf{p}$ is specified in the coordinate frame resulting from the first rotation $\mathbf{q}$. Note that $\mathbf{W}$ is an orthonormal matrix.

C. Kinematics

Let $\mathbf{q}$ describe the rotation from frame X to frame Y and let $\boldsymbol{\omega} = \begin{bmatrix} \omega_x & \omega_y & \omega_z \end{bmatrix}^T$ be the angular velocity of X with respect to Y given in X, then the derivative $\dot{\mathbf{q}}$ is given by

$$\dot{\mathbf{q}} = -\frac{1}{2}\mathbf{W}(\mathbf{q}) \begin{bmatrix} \boldsymbol{\omega} \\ 0 \end{bmatrix} = -\frac{1}{2}\mathbf{W}_R(\mathbf{q})\boldsymbol{\omega} , \tag{4}$$

where $\mathbf{W}_R$ is obtained from $\mathbf{W}$ by deleting the last column.

D. Decomposition into principal rotations

With the modified sign function

$$\overline{\operatorname{sgn}}(a) = \begin{cases} 1 & \text{if} \quad a \geq 0 \\ -1 & \text{if} \quad a < 0 \end{cases} \tag{5}$$

and a given quaternion $\mathbf{q}$ mapping X on Y it is clear from the preceding discussion that $\hat{\mathbf{q}} = \overline{\operatorname{sgn}}(q_4) \cdot \mathbf{q}$ represents the same mapping but with $\hat{\alpha} = 2 \cdot \arccos(\hat{q}_4) \in [0, \pi]$ being the smallest possible rotation angle. With that in mind, we decompose $\mathbf{q}$ into a product of two quaternions $\mathbf{q}_{xy}$ and $\mathbf{q}_z$,

$$\mathbf{q} = \hat{\mathbf{q}} \cdot \overline{\operatorname{sgn}}(q_4) = (\mathbf{q}_{xy} \circ \mathbf{q}_z) \cdot \overline{\operatorname{sgn}}(q_4) . \tag{6}$$

The quaternion $\mathbf{q}_{xy}$ is used to indicate how the z-axis of Y is tilted against the z-axis of X. As shown in Fig. 2, it parametrizes a rotation through an angle φ about an axis $\mathbf{e}_\varphi$

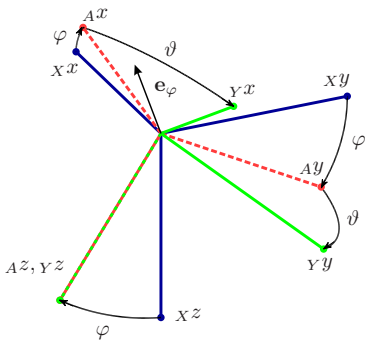

Fig. 2. Initial coordinate system X, auxiliary coordinate system A and target coordinate system Y.

in the xy-plane mapping from X to an auxiliary frame A. The second quaternion $\mathbf{q}_z$ describes the remaining rotation through an angle ϑ about the z-axis mapping from A on Y. Accordingly, $\mathbf{q}_{xy}$ and $\mathbf{q}_z$ are of the structure

$$\mathbf{q}_{xy} = \begin{bmatrix} q_x & q_y & 0 & q_p \end{bmatrix}^T, \quad \mathbf{q}_z = \begin{bmatrix} 0 & 0 & q_z & q_w \end{bmatrix}^T \tag{7}$$

and the corresponding angles are

$$\varphi = 2\arccos(q_p) \quad \text{and} \quad \vartheta = 2\arccos(q_w). \tag{8}$$

Using (7) and (3), the product (6) can be written as

$$\mathbf{q} = \begin{bmatrix} q_w q_x + q_z q_y & q_w q_y - q_z q_x & q_z q_p & q_w q_p \end{bmatrix}^T \cdot \overline{\operatorname{sgn}}(q_4). \tag{9}$$

Since $q_w q_p \geq 0$ holds and since we define $q_p \geq 0$, we also establish $q_w \geq 0$, which means that $\varphi, \vartheta \in [0, \pi]$. Note that the decomposition (6) is not unique if $\mathbf{q} = \begin{bmatrix} q_1 & q_2 & 0 & 0 \end{bmatrix}^T \Leftrightarrow \varphi = \pi$. Then, for any quaternion $\mathbf{q}_{xy} = \begin{bmatrix} q_x & q_y & 0 & 0 \end{bmatrix}^T$ there can be found a suitable $\mathbf{q}_z$ and thus a suitable ϑ such that (6) is fulfilled and vice versa. As long as neither $q_p = 0$ nor $q_w = 0$ the time derivatives of $\mathbf{q}_{xy}$ and $\mathbf{q}_z$ read

$$\dot{\mathbf{q}}_{xy} = \begin{bmatrix} \dot{q}_x \\ \dot{q}_y \\ 0 \\ \dot{q}_p \end{bmatrix} = \frac{1}{2} \begin{bmatrix} \frac{q_y^2 - q_p^2}{q_p} & -\frac{q_x q_y}{q_p} & 2q_y \\ -\frac{q_x q_y}{q_p} & \frac{q_x^2 - q_p^2}{q_p} & -2q_x \\ 0 & 0 & 0 \\ q_x & q_y & 0 \end{bmatrix} \boldsymbol{\omega} , \tag{10}$$

$$\dot{\mathbf{q}}_z = \begin{bmatrix} 0 \\ 0 \\ \dot{q}_z \\ \dot{q}_w \end{bmatrix} = \frac{1}{2q_p} \begin{bmatrix} 0 & 0 & 0 \\ 0 & 0 & 0 \\ -q_w q_y & q_w q_x & -q_w q_p \\ q_z q_y & -q_z q_x & q_z q_p \end{bmatrix} \boldsymbol{\omega} . \tag{11}$$

They follow from (7), (6), (3), (4), $(\mathbf{q}_{xy})_3 \equiv 0$, and the exploitation of the unit length of the quaternions.

III. PROBLEM STATEMENT AND PLANT MODEL

Let the attitude of the quadrotor helicopter be given by the quaternion $\mathbf{q}_b$ mapping the inertial frame N on the body-fixed frame B. Then the objective is to design a control law which aligns frame B with a desired frame D, whose orientation with respect to N is specified by a constant quaternion $\mathbf{q}_d$. According to (3) and (2),

$$\mathbf{q} = \bar{\mathbf{q}}_b \circ \mathbf{q}_d \tag{12}$$

is the rotation error between the frames B and D. With $\boldsymbol{\omega}$ being the angular velocity of the quadrotor helicopter given in B, the control objective can thus be formulated as

$$\mathbf{q} \to \begin{bmatrix} 0 & 0 & 0 & \pm 1 \end{bmatrix}^T , \quad \boldsymbol{\omega} \to \mathbf{0} \quad \text{as} \quad t \to \infty . \tag{13}$$

A decomposition of the error quaternion, as in (6),

$$\mathbf{q} = (\mathbf{q}_{xy} \circ \mathbf{q}_z) \cdot \overline{\operatorname{sgn}}(q_4) \tag{14}$$

reveals that $\mathbf{q}_{xy}$ represents the error between the current and the desired thrust direction, whereas $\mathbf{q}_z$ describes the rotation error around the thrust axis. With (9) and (8) the equivalences

$$\mathbf{q} = \begin{bmatrix} 0 & 0 & 0 & \pm 1 \end{bmatrix}^T \Leftrightarrow \mathbf{q}_{xy} = \mathbf{q}_z = \begin{bmatrix} 0 & 0 & 0 & 1 \end{bmatrix}^T \Leftrightarrow \varphi = \vartheta = 0 \tag{15}$$

can be identified.

Regarding the quadrotor helicopter as a rigid body and neglecting the weak gyroscopic effects of the rotors, the attitude error dynamics are given by

$$\dot{\mathbf{q}} = -\frac{1}{2}\mathbf{W}_R(\mathbf{q})\boldsymbol{\omega}\,, \tag{16}$$

$$\dot{\boldsymbol{\omega}} = \mathbf{J}^{-1}(\mathbf{J}\boldsymbol{\omega}\times\boldsymbol{\omega}) + \mathbf{J}^{-1}\boldsymbol{\tau}\,, \tag{17}$$

where $\mathbf{x} = \begin{bmatrix}\mathbf{q} & \boldsymbol{\omega}\end{bmatrix}^T \in \mathcal{X}$ is the state vector with $\mathcal{X} = \mathcal{S}^3 \times \mathbb{R}^3$, $\mathbf{J} = \mathbf{J}^T > \mathbf{0}$ is the moment of inertia matrix given in B, and $\boldsymbol{\tau} = \begin{bmatrix}\tau_x & \tau_y & \tau_z\end{bmatrix}^T$ is the control torque produced by the rotors given in B. For a quadrotor the magnitude of the available control torque in the xy-plane $\boldsymbol{\tau}_{xy} = \begin{bmatrix}\tau_x & \tau_y\end{bmatrix}^T$ is significantly larger than the available control torque in the z-direction τ_z. This is due to the fact that the rotors mainly produce forces in the negative body-fixed z-direction which, multiplied with their lever arms, give the control torque in the xy-plane. In contrast, the rotors produce only little aerodynamic drag torques around their rotation-axis, which, summed up, give the z-component of the control torque. Thus, we assume that the control torque is bounded as follows:

$$\|\boldsymbol{\tau}_{xy}\| \le \bar{\tau}_{xy}\,, \quad |\tau_z| \le \bar{\tau}_z\,, \tag{18}$$

where $\bar{\tau}_{xy}$ and $\bar{\tau}_z$ are positive constants and $\bar{\tau}_{xy} \gg \bar{\tau}_z$. As will be clarified later, the dynamics of φ are mainly influenced by $\boldsymbol{\tau}_{xy}$. Since moreover the ability of aligning the thrust vector is a crucial requirement for the control of the translational dynamics of a quadrotor, we aim at designing a control law that exploits $\bar{\tau}_{xy}$ as much as possible for a fast reduction of φ. This prioritization leads to a more or less sequential completion of the attitude control task.

IV. CONTROLLER DESIGN

In order to describe the proposed attitude controller, we first introduce some functions. The first function $\Lambda_{\zeta_l}^{\zeta_u} : [0,\pi] \to [0,\zeta_l]$ is defined as

$$\Lambda_{\zeta_l}^{\zeta_u}(\zeta) = \begin{cases} \zeta & \text{if } 0 \le \zeta \le \zeta_l \\ \zeta_l & \text{if } \zeta_l < \zeta \le \zeta_u \\ \zeta_l \cdot \frac{\zeta-\pi}{\zeta_u-\pi} & \text{if } \zeta_u < \zeta \le \pi \end{cases}, \tag{19}$$

where ζ_l and ζ_u are positive constants. $\Lambda_{\zeta_l}^{\zeta_u}$ linearly increases from zero to ζ_l, is then followed by a plateau until ζ_u and then linearly decreases to zero again. Furthermore, we use the function

$$\chi_{\zeta_1}^{\zeta_2}(\zeta,\psi_1(\mathbf{x}),\psi_2(\mathbf{x})) = \begin{cases} \psi_1(\mathbf{x}) & \text{if } \zeta \le \zeta_1 \\ \left(\frac{\zeta_2-\zeta}{\zeta_2-\zeta_1}\right)\psi_1(\mathbf{x}) + \left(\frac{\zeta-\zeta_1}{\zeta_2-\zeta_1}\right)\psi_2(\mathbf{x}) & \text{if } \zeta_1 < \zeta \le \zeta_2 \\ \psi_2(\mathbf{x}) & \text{if } \zeta_2 < \zeta \end{cases}, \tag{20}$$

which provides a linear interpolation between the scalar functions $\psi_1(\mathbf{x})$ and $\psi_2(\mathbf{x})$ with respect to $\zeta \in \mathbb{R}$. Finally, for $\zeta_1 < \zeta_2 < \zeta_3 < \zeta_4$ we define $\chi_{\zeta_1,\zeta_2}^{\zeta_3,\zeta_4}(\zeta,\psi_1(\mathbf{x}),\psi_2(\mathbf{x})) := \chi_{\zeta_1}^{\zeta_2}\left(\zeta,\psi_1(\mathbf{x}),\chi_{\zeta_3}^{\zeta_4}(\zeta,\psi_2(\mathbf{x}),\psi_1(\mathbf{x}))\right)$ which provides a linear interpolation from $\psi_1(\mathbf{x})$ to $\psi_2(\mathbf{x})$ and back to $\psi_1(\mathbf{x})$.

A. Shaping of the Potential Energy

The design of the controller is based on the energy shaping approach as described e.g. in [10]. Since the attitude dynamics are fully actuated this design scheme is easy to apply and offers a transparent physical interpretation. The overall energy of the plant consists only of the rotational energy E_{rot}. By adding an artificial potential energy E_{pot}, we shape the energy of the closed loop system such that it is given by a C^1-function

$$V(\mathbf{x}) = E_{rot}(\boldsymbol{\omega}) + E_{pot}(\mathbf{q}) = \frac{1}{2}\boldsymbol{\omega}^T\mathbf{J}\boldsymbol{\omega} + E_{pot}(\mathbf{q})\,, \tag{21}$$

which satisfies $V(\mathbf{x}_{di}) = 0$ at the desired equilibrium points $\mathbf{x}_{d1}$ and $\mathbf{x}_{d2}$ defined in (13) and $V(\mathbf{x}) > 0$ elsewhere. Note that the sublevel sets of V are compact, since E_{rot} is radially unbounded and since the attitude space itself is compact. Computing $\dot{V}$, we get

$$\begin{aligned}\dot{V}(\mathbf{x}) &= \boldsymbol{\omega}^T\mathbf{J}\dot{\boldsymbol{\omega}} + \frac{\partial E_{pot}(\mathbf{q})}{\partial \mathbf{q}}\dot{\mathbf{q}} \\ &= \boldsymbol{\omega}^T\boldsymbol{\tau} - \underbrace{\frac{1}{2}\frac{\partial E_{pot}(\mathbf{q})}{\partial \mathbf{q}}\mathbf{W}_R(\mathbf{q})}_{\mathbf{T}(\mathbf{q})^T}\boldsymbol{\omega}\,,\end{aligned} \tag{22}$$

where we can identify $\mathbf{T}(\mathbf{q})$ as the torque field resulting from $E_{pot}(\mathbf{q})$. By choosing a control law

$$\boldsymbol{\tau} = \mathbf{T}(\mathbf{q}) - \mathbf{D}(\mathbf{x})\boldsymbol{\omega}\,, \tag{23}$$

where $\mathbf{D}(\mathbf{x}) \ge 0$ is a damping matrix, (22) simplifies to

$$\dot{V}(\mathbf{x}) = -\boldsymbol{\omega}^T\mathbf{D}(\mathbf{x})\boldsymbol{\omega} \le 0. \tag{24}$$

It follows that the compact sublevel sets of V are positively invariant or in other words stability of the desired attitude. In order to prove asymptotic stability, we apply the Krasovskii-LaSalle invariance principle in Section V.

To shape the energy, we assign a potential energy function

$$E_{pot}(\varphi,\vartheta) = E_\varphi(\varphi) + E_\vartheta(\varphi,\vartheta)\,, \tag{25}$$

$$\text{where} \quad E_\varphi(\varphi) = c_\varphi \int_0^\varphi \Lambda_{\varphi_l}^{\varphi_u}(\zeta)\, d\zeta\,, \tag{26}$$

$$E_\vartheta(\varphi,\vartheta) = \cos^4\!\left(\frac{\varphi}{2}\right)\cdot c_\vartheta \int_0^\vartheta \Lambda_{\vartheta_l}^{\vartheta_u}(\zeta)\, d\zeta \tag{27}$$

and c_φ, c_ϑ are positive constants. The potential energy E_{pot} given above is constructed such that it exhibits its only minimum at $(\varphi,\vartheta) = (0,0)$ and (considering the non-uniqueness of ϑ at $\varphi = \pi$) its maximum value for $(\varphi,\vartheta) = (\pi,\vartheta)$. One more critical point is located at $(\varphi,\vartheta) = (0,\pi)$. To exclude further critical points one has to parametrize E_φ and E_ϑ, such that

$$\frac{\partial E_{pot}(\varphi,\vartheta)}{\partial\varphi} = \frac{\partial E_\varphi(\varphi)}{\partial\varphi} + \frac{\partial E_\vartheta(\varphi,\vartheta)}{\partial\varphi} > 0 \tag{28}$$

holds for $(\varphi,\vartheta) \in\,]0,\pi[\times[0,\pi]$. In order to motivate the choice of the potential energy, it is helpful to analyze the torque field that it generates. As in (22), $\dot{E}_{pot}$ is calculated to identify the torque $\mathbf{T}$,

$$\dot{E}_{pot}(\mathbf{x}) = \tfrac{\partial E_{pot}(\varphi,\vartheta)}{\partial\varphi}\dot{\varphi} + \tfrac{\partial E_{pot}(\varphi,\vartheta)}{\partial\vartheta}\dot{\vartheta} = -\mathbf{T}^T(\mathbf{q})\boldsymbol{\omega}. \tag{29}$$

Using (8), (10) and (11), the time derivatives $\dot{\varphi}$ and $\dot{\vartheta}$ read

$$\dot{\varphi} = -\mathbf{e}_{\varphi}^T \boldsymbol{\omega}, \quad \dot{\vartheta} = -\frac{q_z}{\sqrt{1-q_w^2}} \left(\frac{\sqrt{1-q_p^2}}{q_p} \mathbf{e}_{\perp}^T + \mathbf{e}_z^T \right) \boldsymbol{\omega}. \quad (30)$$

Here, $\mathbf{e}_{\varphi}$, $\mathbf{e}_{\perp}$ and $\mathbf{e}_z$ denote the unit vectors

$$\mathbf{e}_{\varphi} = \frac{1}{\sqrt{1-q_p^2}} \begin{bmatrix} q_x \\ q_y \\ 0 \end{bmatrix}, \; \mathbf{e}_{\perp} = \frac{1}{\sqrt{1-q_p^2}} \begin{bmatrix} q_y \\ -q_x \\ 0 \end{bmatrix}, \; \mathbf{e}_z = \begin{bmatrix} 0 \\ 0 \\ 1 \end{bmatrix}, \quad (31)$$

which span an orthonormal basis of $\mathbb{R}^3$. By inserting (30) and (31) into (29), the torque $\mathbf{T}$ is obtained. We further decompose $\mathbf{T}$ into parts according to the corresponding energy components E_{φ} and E_{ϑ} and their effective directions $\mathbf{e}_{\varphi}$, $\mathbf{e}_{\perp}$ and $\mathbf{e}_z$. This results in

$$\mathbf{T}(\mathbf{q}) = \underbrace{\mathbf{T}_{\varphi}^{\varphi}(\mathbf{q}) + \mathbf{T}_{\varphi}^{\vartheta}(\mathbf{q}) + \mathbf{T}_{\perp}^{\vartheta}(\mathbf{q})}_{\begin{bmatrix} \mathbf{T}_{xy}^T & 0 \end{bmatrix}^T} + \underbrace{\mathbf{T}_{z}^{\vartheta}(\mathbf{q})}_{\begin{bmatrix} 0 & 0 & T_z \end{bmatrix}^T} \quad (32)$$

where

$$\begin{aligned} \mathbf{T}_{\varphi}^{\varphi}(\mathbf{q}) &= \tfrac{\partial E_{\varphi}(\varphi)}{\partial \varphi} \mathbf{e}_{\varphi}, \quad \mathbf{T}_{\perp}^{\vartheta}(\mathbf{q}) = \tfrac{\partial E_{\vartheta}(\varphi,\vartheta)}{\partial \vartheta} \tfrac{q_z \sqrt{1-q_p^2}}{q_p \sqrt{1-q_w^2}} \mathbf{e}_{\perp}, \\ \mathbf{T}_{\varphi}^{\vartheta}(\mathbf{q}) &= \tfrac{\partial E_{\vartheta}(\varphi,\vartheta)}{\partial \varphi} \mathbf{e}_{\varphi}, \; \mathbf{T}_{z}^{\vartheta}(\mathbf{q}) = \tfrac{\partial E_{\vartheta}(\varphi,\vartheta)}{\partial \vartheta} \tfrac{q_z}{\sqrt{1-q_w^2}} \mathbf{e}_z. \end{aligned} \quad (33)$$

Using (26), (27), and (8), we can rewrite (33) as

$$\begin{aligned} \mathbf{T}_{\varphi}^{\varphi} &= c_{\varphi} \Lambda_{\varphi_l}^{\varphi_u}(\varphi)\, \mathbf{e}_{\varphi}, \\ \mathbf{T}_{\varphi}^{\vartheta} &= -\cos^3(\tfrac{\varphi}{2}) \sin(\tfrac{\varphi}{2}) \cdot c_{\vartheta} \int_0^{\vartheta} \Lambda_{\vartheta_l}^{\vartheta_u}(\zeta)\; d\zeta \cdot \mathbf{e}_{\varphi}, \\ \mathbf{T}_{\perp}^{\vartheta} &= \tfrac{q_z}{\sqrt{1-q_w^2}} \cos^3(\tfrac{\varphi}{2}) \sin(\tfrac{\varphi}{2}) \cdot c_{\vartheta} \Lambda_{\vartheta_l}^{\vartheta_u}(\vartheta)\, \mathbf{e}_{\perp}, \\ \mathbf{T}_{z}^{\vartheta} &= \tfrac{q_z}{\sqrt{1-q_w^2}} \cos^4(\tfrac{\varphi}{2}) \cdot c_{\vartheta} \Lambda_{\vartheta_l}^{\vartheta_u}(\vartheta)\, \mathbf{e}_z. \end{aligned} \quad (34)$$

The chosen potential energy function (25) extends the potential energy E_{φ}, introduced in [5], by a further component E_{ϑ}. The energy E_{φ} can be thought of as the potential caused by a saturating torsion spring arranged between the actual and the desired thrust direction. Accordingly, it generates a torque $\mathbf{T}_{\varphi}^{\varphi}$ depending only on φ, which ensures the alignment of the body-fixed z-axis. See [5] for a detailed discussion. The energy component E_{ϑ} serves to generate control torques that reduce the error angle ϑ defined about the desired thrust axis. In detail, the torques $\mathbf{T}_z^{\vartheta}$, $\mathbf{T}_{\perp}^{\vartheta}$ and $\mathbf{T}_{\varphi}^{\vartheta}$ are induced by E_{ϑ} and their influence decays with increasing φ. While $\mathbf{T}_z^{\vartheta}$ can be regarded as the "intended" torque, which for a constant φ, acts around the z-axis analogous to $\mathbf{T}_{\varphi}^{\varphi}$, the components $\mathbf{T}_{\perp}^{\vartheta}$ and $\mathbf{T}_{\varphi}^{\vartheta}$ can be considered "parasitic". This is because $\mathbf{T}_{\varphi}^{\vartheta}$ always counteracts $\mathbf{T}_{\varphi}^{\varphi}$ and $\mathbf{T}_{\perp}^{\vartheta}$ induces a motion around $\mathbf{e}_{\perp}$, which does not contribute to a decrease of φ according to (30). At the same time, $\mathbf{T}_{\perp}^{\vartheta}$ reduces the available control authority for $\mathbf{T}_{\varphi}^{\varphi}$, since in view of (18)

$$\|\mathbf{T}_{xy}\| = \sqrt{(\|\mathbf{T}_{\varphi}^{\varphi}\| - \|\mathbf{T}_{\varphi}^{\vartheta}\|)^2 + \|\mathbf{T}_{\perp}^{\vartheta}\|^2} < \bar{\tau}_{xy} \quad \forall \varphi, \vartheta \quad (35)$$

must hold. Just like compliance with (28) (which in turn is equivalent to $\|\mathbf{T}_{\varphi}^{\varphi}\| - \|\mathbf{T}_{\varphi}^{\vartheta}\| > 0$) is a matter of parametrizing E_{pot} the same holds for guaranteeing (35) and

$$|T_z| = \|\mathbf{T}_z^{\vartheta}\| < \bar{\tau}_z \quad \forall \varphi, \vartheta, \quad (36)$$

which is the second constraint arising from (18). Note that we formulate (35) and (36) as strict inequalities in order to reserve some control torque for damping purposes. Note also that E_{pot} is constructed, such that no discontinuities in $\mathbf{T}$ occur in particular at states where $\varphi = \pi$ or $\vartheta = \pi$.

B. Damping Injection

We complete the control law (23) with a damping matrix

$$\begin{aligned} \mathbf{D}(\mathbf{x}) &= \kappa_{xy}(\mathbf{x}) \big(d_{\varphi}(\mathbf{x}) \mathbf{e}_{\varphi} \mathbf{e}_{\varphi}^T + d_{\perp} \mathbf{e}_{\perp} \mathbf{e}_{\perp}^T \big) + \kappa_z(\mathbf{x}) d_z(\mathbf{x}) \mathbf{e}_z \mathbf{e}_z^T \\ &= \begin{bmatrix} \kappa_{xy}(\mathbf{x}) \mathbf{D}_{xy}(\mathbf{x}) & \mathbf{0} \\ \mathbf{0} & \kappa_z(\mathbf{x}) d_z(\mathbf{x}) \end{bmatrix} \geq 0, \end{aligned} \quad (37)$$

which is composed of the damping coefficients $d_{\varphi}(\mathbf{x})$, $d_{\perp}$ and $d_z(\mathbf{x})$. They allow an individual damping of the angular velocity components $\omega_{\varphi} = \mathbf{e}_{\varphi}^T \boldsymbol{\omega} = -\dot{\varphi}$, $\omega_{\perp} = \mathbf{e}_{\perp}^T \boldsymbol{\omega}$ and $\omega_z = \mathbf{e}_z^T \boldsymbol{\omega}$, which are obtained by projecting $\boldsymbol{\omega}$ on the basis vectors given in (31). The submatrix $\mathbf{D}_{xy}(\mathbf{x})$ in (37) reads

$$\mathbf{D}_{xy}(\mathbf{x}) = \tfrac{d_{\varphi}(\mathbf{x})}{1-q_p^2} \begin{bmatrix} q_x^2 & q_x q_y \\ q_x q_y & q_y^2 \end{bmatrix} + \tfrac{d_{\perp}}{1-q_p^2} \begin{bmatrix} q_y^2 & -q_x q_y \\ -q_x q_y & q_x^2 \end{bmatrix} \quad (38)$$

and the gains $\kappa_{xy}(\mathbf{x})$ and $\kappa_z(\mathbf{x})$ serve to saturate the damping torques if necessary. They are defined as

$$\begin{aligned} \kappa_{xy}(\mathbf{x}) &= \min_{\kappa > 0, \|\mathbf{T}_{xy} - \kappa \cdot \mathbf{D}_{xy} \boldsymbol{\omega}_{xy}\| = \bar{\tau}_{xy}} (1, \kappa), \\ \kappa_z(\mathbf{x}) &= \min_{\kappa > 0, |T_z - \kappa \cdot d_z \omega_z| = \bar{\tau}_z} (1, \kappa), \end{aligned} \quad (39)$$

where $\boldsymbol{\omega}_{xy} = \begin{bmatrix} \omega_x & \omega_y \end{bmatrix}^T$. The choice of the damping coefficients $d_{\varphi}(\mathbf{x})$, $d_{\perp}$ and $d_z(\mathbf{x})$ given below is motivated by some assumptions on the motion of the controlled system and on the inertia matrix $\mathbf{J}$. These assumptions serve only to facilitate the design of the damping, but are not required to derive the stability properties of the closed loop.

Regarding the symmetry of a quadrotor, we assume a diagonal inertia matrix $\hat{\mathbf{J}} = \operatorname{diag}(\hat{\mathbf{J}}_1, \hat{\mathbf{J}}_1, \hat{\mathbf{J}}_2)$. Moreover, since $\bar{\tau}_{xy} >> \bar{\tau}_z$ and since $\bar{\tau}_{xy}$ is mainly exploited to reduce φ, we assume a sequential completion of the control task. This means that first φ is driven to zero while ϑ remains more or less constant and only afterwards ϑ is reduced to zero. This implies that in the first phase the simplifying assumption $\dot{\boldsymbol{\omega}} \parallel \boldsymbol{\omega} \parallel \mathbf{e}_{\varphi}$ is justified and provided that $\kappa_{xy} = 1$, the scalar differential equation

$$\hat{J}_1 \ddot{\varphi} = -T_{\varphi} - d_{\varphi}(\mathbf{x}) \cdot \dot{\varphi} \quad (40)$$

approximately holds, where $T_{\varphi} = \|\mathbf{T}_{\varphi}^{\varphi}\| - \|\mathbf{T}_{\varphi}^{\vartheta}\| \geq 0$. It can be seen from (34) that near $\varphi = 0$ the torque T_{φ} can be considered linear in φ. Thus, if φ_l is sufficiently small, (40) approximately becomes

$$\hat{J}_1 \ddot{\varphi} = -c \cdot \varphi - d_{\varphi}(\mathbf{x}) \cdot \dot{\varphi} \quad \text{if} \quad 0 < \varphi \leq \varphi_l, \quad (41)$$

where $c \leq c_{\varphi}$ is a positive constant. By choosing

$$d_{\varphi}(\mathbf{x}) = \chi_{\varphi_l,\, \varphi_l + \Delta\varphi}^{\varphi_u - \Delta\varphi,\, \varphi_u}(\varphi, \delta_{\varphi}, d_{\varphi}^*(\mathbf{x})), \quad (42)$$

where δ_{φ} and $\Delta\varphi$ are positive constants, the dynamics (41) are rendered linear. A sophisticated damping strategy $d_{\varphi}^*(\mathbf{x})$ is applied in the region $\varphi \in \Phi = \{\varphi : \varphi_l + \Delta\varphi < \varphi < \varphi_u - \Delta\varphi\}$. There, a strategy similar to the bang-bang solution

of a time optimal control is applied. This requires to indicate a switching curve $s_\varphi(\varphi) < 0$ where the transition from acceleration ($\ddot{\varphi} < 0$) to deceleration ($\ddot{\varphi} > 0$) occurs. If $\dot{\varphi} > s(\varphi)$, the damping $d^*_\varphi(\mathbf{x})$ is chosen to enable maximum acceleration based on (40). In case of $\dot{\varphi} > 0$, this means supporting the torque $-T_\varphi$ by a positive damping $d^*_\varphi(\mathbf{x}) > 0$, such that the maximum torque $\bar{\tau}_{xy}$ is exploited. In case of $\dot{\varphi} < 0$, the damping is set to zero to avoid counteracting $-T_\varphi$. If $\dot{\varphi} < s(\varphi) < 0$ maximum deceleration is desired, which can be achieved by choosing $d^*_\varphi(\mathbf{x}) > 0$ so high that $-T_\varphi$ is overcompensated and $\bar{\tau}_{xy}$ is used to slow down. Summing up, we choose

$$d^*_\varphi(\mathbf{x}) = \chi^{r_\varphi \cdot s_\varphi(\varphi)}_{s_\varphi(\varphi)}\left(\dot{\varphi}, d^*_{\varphi dec}(\mathbf{x}), d^*_{\varphi acc}(\mathbf{x})\right), \tag{43}$$

$$\text{where} \quad d^*_{\varphi acc}(\mathbf{x}) = \begin{cases} -\frac{T_\varphi}{\dot{\varphi}} + \frac{\bar{\tau}_{xy}}{\dot{\varphi}} & \text{if } \dot{\varphi} > v_\varphi \\ -\frac{T_\varphi}{v_\varphi} + \frac{\bar{\tau}_{xy}}{v_\varphi} & \text{if } v_\varphi \geq \dot{\varphi} > 0 \\ 0 & \text{if } 0 \geq \dot{\varphi}, \end{cases} \tag{44}$$

$$d^*_{\varphi dec}(\mathbf{x}) = -\frac{T_\varphi}{\dot{\varphi}} - \frac{\bar{\tau}_{xy}}{\dot{\varphi}} \tag{45}$$

and r_φ as well as v_φ are positive constants. It is clear from (43) that $0 < r_\varphi < 1$ defines a region of interpolation between acceleration and deceleration in order to render the resulting torque continuous. An examination of (44) reveals that the small constant $v_\varphi > 0$ prevents the damping from growing unbounded when $\dot{\varphi}$ approaches zero. The switching curve we use in (43) reads

$$s_\varphi(\varphi) = -\sqrt{v^2_{\varphi max} - 2\hat{J}_1^{-1}\bar{\tau}_{xy}(\varphi_l - \varphi)} < 0 \tag{46}$$

and is the phase-plane trajectory $\dot{\varphi}(\varphi)$ solving $\hat{J}_1\ddot{\varphi} = \bar{\tau}_{xy}$ and entering $\varphi \leq \varphi_l$ with a velocity $\dot{\varphi} = -v_{\varphi max} < 0$.

For the damping influencing $\omega_\perp$ we simply choose

$$d_\perp = \delta_\varphi \tag{47}$$

to be constant. Note that according to (42) and (38) this ensures that $\mathbf{D}_{xy}(\mathbf{x}) = \mathrm{diag}(\delta_\varphi, \delta_\varphi) > 0$ if $\varphi < \varphi_l$ or $\varphi > \varphi_u$ and this way effectively omits difficulties with determining $\mathbf{e}_\varphi$ and $\mathbf{e}_\perp$ near $\varphi = 0$ and $\varphi = \pi$.

The damping $d_z(\mathbf{x})$ is designed analogously to $d_\varphi(\mathbf{x})$ based on the dynamics

$$\hat{J}_2\ddot{\vartheta} = -|T_z| - d_z(\mathbf{x}) \cdot \dot{\vartheta}, \tag{48}$$

which result from the assumptions that $\kappa_z(\mathbf{x}) = 1$ and that the first phase, the alignment of the thrust direction, is terminated. Thus $\varphi \equiv 0$ and consequently $\dot{\boldsymbol{\omega}} \parallel \boldsymbol{\omega} \parallel \mathbf{e}_z$ holds. Explicitely, the damping $d_z(\mathbf{x})$ is

$$d_z(\mathbf{x}) = \chi^{\varphi_u}_{\varphi_u - \Delta\varphi}\left(\varphi, \chi^{\vartheta_u - \Delta\vartheta,\, \vartheta_u}_{\vartheta_l,\, \vartheta_l + \Delta\vartheta}(\vartheta, \delta_z, d^*_z(\mathbf{x})), \delta_z\right), \tag{49}$$

where $\Delta\vartheta$ and δ_z are positive constants. Note that the additional outer interpolation function is necessary to account for the non-uniqueness of ϑ if $\varphi = \pi$. Again, the dynamics (48) are rendered linear for $0 < \vartheta \leq \vartheta_l$, where $|T_z| = c_\vartheta\vartheta$. The damping $d^*_z(\mathbf{x})$, which is active for $\vartheta \in \Theta = \{\vartheta : \vartheta_l + \Delta\vartheta < \vartheta < \vartheta_u - \Delta\vartheta\}$ and $\varphi < \varphi_u + \Delta\varphi$, is given by

$$d^*_z(\mathbf{x}) = \chi^{r_\vartheta \cdot s_\vartheta(\vartheta)}_{s_\vartheta(\vartheta)}(\dot{\vartheta}, d^*_{zdec}(\mathbf{x}), d^*_{zacc}(\mathbf{x})). \tag{50}$$

The corresponding switching curve is

$$s_\vartheta(\vartheta) = -\sqrt{v^2_{\vartheta max} - 2\hat{J}_2^{-1}\bar{\tau}_z(\vartheta_l - \vartheta)} < 0, \tag{51}$$

the damping used for acceleration and deceleration reads

$$d^*_{zacc}(\mathbf{x}) = \begin{cases} -\frac{|T_z|}{\mathring{\vartheta}_z} + \frac{\bar{\tau}_z}{\mathring{\vartheta}_z} & \text{if } \mathring{\vartheta}_z > v_\vartheta \\ -\frac{|T_z|}{v_\vartheta} + \frac{\bar{\tau}_z}{v_\vartheta} & \text{if } v_\vartheta \geq \mathring{\vartheta}_z > 0 \\ 0 & \text{if } 0 \geq \mathring{\vartheta}_z, \end{cases} \tag{52}$$

$$d^*_{zdec}(\mathbf{x}) = \begin{cases} -\frac{|T_z|}{\mathring{\vartheta}_z} - \frac{\bar{\tau}_z}{\mathring{\vartheta}_z} & \text{if } \mathring{\vartheta}_z < -v_\vartheta \\ -\frac{|T_z|}{v_\vartheta} - \frac{\bar{\tau}_z}{v_\vartheta} & \text{if } -v_\vartheta \leq \mathring{\vartheta}_z < 0 \\ 0 & \text{if } 0 \leq \mathring{\vartheta}_z \end{cases} \tag{53}$$

and $v_{\vartheta max} > 0$, $v_\vartheta > 0$ and $0 < r_\vartheta < 1$ are constants. Note that we use $\mathring{\vartheta}_z = -\frac{q_z}{\sqrt{1-q_w^2}}\omega_z$ instead of $\dot{\vartheta}$ to distinguish between the cases in (52) and (53). This is done because $d_z(\mathbf{x})$ is only effective in connection with ω_z and according to (30) the quantity $\mathring{\vartheta}_z$ represents the part of $\dot{\vartheta}$ that depends on ω_z. Note moreover that if the assumption $\varphi \equiv 0$, required for (48) to hold, is fulfilled, then $\dot{\vartheta}$ coincides with $\mathring{\vartheta}_z$.

V. STABILITY PROPERTIES

In this section we prove almost global asymptotic stability of the desired attitude by showing first that the set of desired equilibrium points is asymptotically stable and second that all other equilibrium points are unstable. As it is analyzed in [1], almost global asymptotic stability is the best we can achieve with a continuous control law.

By inserting the control law (23) derived in the previous section in the dynamics (16), (17) and setting the left hand side to zero, the equilibrium points of the closed loop system can be identified as the members of the sets

$$\begin{aligned} \mathcal{X}_d &= \left\{\mathbf{x} \in \mathcal{X} : \mathbf{q} = \begin{bmatrix}0 & 0 & 0 & \pm 1\end{bmatrix}^T, \boldsymbol{\omega} = \mathbf{0}\right\}, \\ \mathcal{X}_{u1} &= \left\{\mathbf{x} \in \mathcal{X} : \mathbf{q} = \begin{bmatrix}0 & 0 & \pm 1 & 0\end{bmatrix}^T, \boldsymbol{\omega} = \mathbf{0}\right\}, \\ \mathcal{X}_{u2} &= \left\{\mathbf{x} \in \mathcal{X} : \mathbf{q} = \begin{bmatrix}q_1 & q_2 & 0 & 0\end{bmatrix}^T, \boldsymbol{\omega} = \mathbf{0}\right\}. \end{aligned} \tag{54}$$

$\mathcal{X}_d$ denotes the set of desired equilibrium points, whereas $\mathcal{X}_{u1}$ and $\mathcal{X}_{u2}$ denote the sets of the undesired ones. Note that $\mathbf{x} \in \mathcal{X}_d \Leftrightarrow \varphi = \vartheta = 0$, $\mathbf{x} \in \mathcal{X}_{u1} \Leftrightarrow \varphi = 0, \vartheta = \pi$ and $\mathbf{x} \in \mathcal{X}_{u2} \Leftrightarrow \varphi = \pi$ holds. In order to apply the Krasovskii-LaSalle invariance principle one first has to determine the set $\mathcal{E} := \{\mathbf{x} \in \mathcal{X} \,|\, \dot{V}(\mathbf{x}) = 0\}$ in which the time derivative $\dot{V}$ is zero. Inserting (37) in (24) and remembering that $\kappa_{xy}(\mathbf{x}) > 0$ and $\kappa_z(\mathbf{x}) > 0$ shows that

$$\dot{V}(\mathbf{x}) = -\kappa_{xy}(\mathbf{x})\left(d_\varphi(\mathbf{x})\omega^2_\varphi + d_\perp\omega^2_\perp\right) - \kappa_z(\mathbf{x})d_z(\mathbf{x})\omega^2_z \tag{55}$$

only vanishes if $d_\varphi(\mathbf{x})\omega^2_\varphi = d_\perp\omega^2_\perp = d_z(\mathbf{x})\omega^2_z = 0$ holds. Outside the equilibrium points, in the set $\tilde{\mathcal{X}} := \mathcal{X}\backslash(\mathcal{X}_d \cup \mathcal{X}_{u1} \cup \mathcal{X}_{u2})$, this condition is only fulfilled in the subset $\mathcal{E}_1$, which is the set of all states with zero angular velocity, and in the sets $\mathcal{E}_2$, $\mathcal{E}_3$, $\mathcal{E}_4$, in which $\boldsymbol{\omega} \neq \mathbf{0}$ while $\omega_\perp = d_\varphi(\mathbf{x})\omega^2_\varphi = d_z(\mathbf{x})\omega^2_z = 0$. Thus, the sets $\mathcal{E}_2$, $\mathcal{E}_3$, $\mathcal{E}_4$ are subsets of the state space regions where $d_\varphi(\mathbf{x}) = 0$ or $d_z(\mathbf{x}) = 0$. Explicitly stated, the sets $\mathcal{E}_1$,$\mathcal{E}_2$, $\mathcal{E}_3$, $\mathcal{E}_4$ are

$$\mathcal{E}_1 = \left\{\mathbf{x} \in \tilde{\mathcal{X}} : \boldsymbol{\omega} = \mathbf{0}\right\},$$

$$\mathcal{E}_2 = \Big\{\mathbf{x}\in\tilde{\mathcal{X}} : \varphi\in\Phi, \vartheta\in\Theta, \boldsymbol{\omega} = \alpha\mathbf{e}_\varphi + \tfrac{q_z}{\sqrt{1-q_w^2}}\beta\mathbf{e}_z \neq \mathbf{0},$$
$$0\leq\alpha\leq -r_\varphi s_\varphi(\varphi), 0\leq\beta\leq -r_\vartheta s_\vartheta(\vartheta)\Big\},$$
$$\mathcal{E}_3 = \Big\{\mathbf{x}\in\tilde{\mathcal{X}} : \varphi\in\Phi, \vartheta\notin\Theta, \boldsymbol{\omega} = \alpha\mathbf{e}_\varphi,$$
$$0<\alpha\leq -r_\varphi s_\varphi(\varphi), \Big\},$$
$$\mathcal{E}_4 = \Big\{\mathbf{x}\in\tilde{\mathcal{X}} : \varphi\leq\varphi_l+\Delta\varphi, \vartheta\in\Theta, \boldsymbol{\omega} = \tfrac{q_z}{\sqrt{1-q_w^2}}\beta\mathbf{e}_z,$$
$$0<\beta\leq -r_\vartheta s_\vartheta(\vartheta)\Big\}.$$

Next, we show that $\mathcal{X}_d$, $\mathcal{X}_{u1}$ and $\mathcal{X}_{u2}$ are the only invariant sets in $\mathcal{E} = \mathcal{E}_1\cup\mathcal{E}_2\cup\mathcal{E}_3\cup\mathcal{E}_4\cup\mathcal{X}_d\cup\mathcal{X}_{u1}\cup\mathcal{X}_{u2}$. Imagine that $\mathbf{x}\in\mathcal{E}_1$, then $\boldsymbol{\tau}\neq\mathbf{0}$ and since $\boldsymbol{\omega}=\mathbf{0}$, we have $\dot{\boldsymbol{\omega}}\neq\mathbf{0}$ from (17). Thus, the state will exit the subset $\mathcal{E}_1$ instantaneously, which shows that no invariant sets are contained in $\mathcal{E}_1$.

If the state of the closed loop system is inside the subset $\mathcal{E}_2$, then no damping occurs and hence using (34) the torque can be identified as $\boldsymbol{\tau} = \mathbf{T} = \mathbf{T}_\varphi^\varphi + \mathbf{T}_\varphi^\vartheta + \mathbf{T}_\perp^\vartheta + \mathbf{T}_z^\vartheta = \mu\cdot\mathbf{e}_\varphi + \nu\cdot\mathbf{e}_\perp + \frac{q_z}{\sqrt{1-q_w^2}}\eta\cdot\mathbf{e}_z$ with $\mu>0$ and $\eta>0$. Based on (46) and (51), an upper bound for α and β is given by

$$L := \max(-s_\varphi(\pi), -s_\vartheta(\pi)) > \max(\alpha,\beta) > 0. \tag{56}$$

A lower bound for the angular velocity $\underline{\omega}$ is received solving

$$E_{rot0} = \frac{1}{2}\boldsymbol{\omega}_0^T\mathbf{J}\boldsymbol{\omega}_0 = \frac{1}{2}\bar{\lambda}(\mathbf{J})\underline{\omega}^2 > 0 \tag{57}$$

in which E_{rot0} is the rotational energy and $\boldsymbol{\omega}_0$ the angular velocity at the time $t=0$ and $\bar{\lambda}(\mathbf{J})$ represents the largest eigenvalue of $\mathbf{J}$. Now as long as $\mathbf{x}\in\mathcal{E}_2$, it holds that $\dot{E}_{rot} = \boldsymbol{\omega}^T\boldsymbol{\tau} = \alpha\mu+\beta\eta > 0$ and consequently

$$0<\underline{\omega}^2\leq\boldsymbol{\omega}^T\boldsymbol{\omega} = \alpha^2+\beta^2 \tag{58}$$

Using (30), one recognizes that $\dot{\varphi} = -\alpha\leq 0$ and since $\omega_\perp = 0$, it holds that $\dot{\vartheta} = -\frac{q_z}{\sqrt{1-q_w^2}}\omega_z = -\beta\leq 0$. Together with (56) we can hence reformulate and extend (58) to obtain

$$0<\underline{\omega}^2\leq\alpha^2+\beta^2 = \alpha(-\dot{\varphi})+\beta(-\dot{\vartheta})\leq -L(\dot{\varphi}+\dot{\vartheta}). \tag{59}$$

Now, let $\varphi_0\in\Phi$ and $\vartheta_0\in\Theta$ be the error angles at $t=0$. The time $\tilde{t}$ solving the equation

$$(\varphi_l+\Delta\varphi)+(\vartheta_l+\Delta\vartheta) = (\varphi_0+\vartheta_0)+\int_0^{\tilde{t}}(\dot{\varphi}+\dot{\vartheta})dt \tag{60}$$

certainly is an upper bound of the time at which the state must leave $\mathcal{E}_2$. By inserting (59) in (60) and evaluating the integral, we obtain the inequality

$$(\varphi_l+\Delta\varphi)+(\vartheta_l+\Delta\vartheta)\leq(\varphi_0+\vartheta_0)-\frac{\underline{\omega}^2}{L}\tilde{t}, \tag{61}$$

which reveals that $\tilde{t}$ itself is upper bounded by

$$\tilde{t}\leq L\frac{(\varphi_0-(\varphi_l+\Delta\varphi))+(\vartheta_0-(\vartheta_l+\Delta\vartheta))}{\underline{\omega}^2}. \tag{62}$$

Note that $\mathcal{E}_2$ might also be left because α, β or $\boldsymbol{\omega}$ violate their constraints. Since $\mathcal{E}_2$ is left in any case, it cannot contain any invariant sets. A similar argumentation holds for $\mathcal{E}_3$ and $\mathcal{E}_4$, but is omitted here due to space limitations. Moreover, also the union of $\mathcal{E}_1$, $\mathcal{E}_2$, $\mathcal{E}_3$ and $\mathcal{E}_4$ cannot contain any invariant sets. Indeed, the state may cross over from $\mathcal{E}_1$ into each of the other sets and also from $\mathcal{E}_2$ to $\mathcal{E}_3$ or $\mathcal{E}_4$ but no other transitions are possible. Hence, the union of the sets of equilibrium points given in (54) is the largest invariant set contained in $\mathcal{E}$ and according to the Krasovskii-LaSalle invariance principle every trajectory converges to $\mathcal{X}_d$, $\mathcal{X}_{u1}$ or $\mathcal{X}_{u2}$.

In order to prove almost global asymptotic stability of $\mathcal{X}_d$, representing the desired attitude, we first notice that $V(\mathbf{x}) = 0, \forall\mathbf{x}\in\mathcal{X}_d$, $V(\mathbf{x}) = E_\vartheta(0,\pi) > 0, \forall\mathbf{x}\in\mathcal{X}_{u1}$ and $V(\mathbf{x}) = E_\varphi(\pi) > 0, \forall\mathbf{x}\in\mathcal{X}_{u2}$. Note that $E_\vartheta(0,\pi) = E_{pot}(0,\pi) < E_\varphi(\pi)$ because $E_\varphi(\pi) = \max(E_{pot}(\varphi,\vartheta))$ and moreover (28) holds. If we choose any initial state $\mathbf{x}_0$, such that $V(\mathbf{x}_0) < E_\vartheta(0,\pi)$, we exclude $\mathcal{X}_{u1}$ and $\mathcal{X}_{u2}$ from the initial sublevel set of $V(\mathbf{x})$ and the solution can only approach $\mathcal{X}_d$. Hence, $\mathcal{X}_d$ is a set of asymptotically stable equilibrium points. Since the set $\{\mathbf{x}\in\mathcal{X}|V(\mathbf{x}) < E_\vartheta(0,\pi)\}$ is adjacent to all members of $\mathcal{X}_{u1}$, the preceding argumentation also proves that the equilibrium points in $\mathcal{X}_{u1}$ are unstable. Now, if we choose any initial state $\mathbf{x}_0$, such that $V(\mathbf{x}_0) < E_\varphi(\pi)$, we exclude $\mathcal{X}_{u2}$ from the initial sublevel set of $V(\mathbf{x})$ and the solution will approach $\mathcal{X}_d$ or $\mathcal{X}_{u1}$. Again, the set $\{\mathbf{x}\in\mathcal{X}|V(\mathbf{x}) < E_\varphi(\pi)\}$ is adjacent to all members of $\mathcal{X}_{u2}$, which consequently are unstable equilibrium points. It follows that the union of all stable manifolds of the unstable equilibrium points contained in $\mathcal{X}_{u1}\cup\mathcal{X}_{u2}$ is of smaller dimension than the state space. It is known that an m-dimensional invariant manifold of an n-dimensional system has Lebesgue measure zero if $m<n$, see e.g. [9]. This proves almost global asymptotic stability of $\mathcal{X}_d$. It is worth noticing that although some assumptions on $\mathbf{J}$ were made during the design process, the proof holds for arbitrary unknown $\mathbf{J}$.

VI. Simulation Results

In order to analyze the performance of the proposed controller 51 simulation runs have been executed. While the controller and the initial conditions were unchanged for all simulations, the plant was varied by changing the moment of inertia matrix $\mathbf{J}$ by adding a symmetric random matrix $\Delta\mathbf{J}$ to a nominal diagonal inertia matrix $\hat{\mathbf{J}}$, which was also used for the controller design. The elements of the uncertainty $\Delta\mathbf{J}$ were constrained by $-0.1\cdot(\hat{\mathbf{J}})_{11}\leq(\Delta\mathbf{J})_{ij}\leq 0.1\cdot(\hat{\mathbf{J}})_{11}$ and the positive definiteness of $\mathbf{J} = \hat{\mathbf{J}}+\Delta\mathbf{J}$. The lines in Fig. 3 correspond to the closed loop system incorporating the nominal plant ($\mathbf{J}=\hat{\mathbf{J}}$), whereas the shaded areas mark the regions which contain the signals resulting from the remaining 50 simulations. All controller and plant parameters are listed in Table I. The initial conditions for the simulations are given by the quaternion $\mathbf{q}_0 = \begin{bmatrix}0.992 & 0.087 & -0.008 & 0.087\end{bmatrix}^T$ corresponding to the error angles $\varphi_0 = 170\frac{\pi}{180}\mathrm{rad}$ and $\vartheta_0 = 10\frac{\pi}{180}\mathrm{rad}$ and the angular velocity $\boldsymbol{\omega}_0 = \begin{bmatrix}0 & 0 & 1.7\end{bmatrix}^T\,\mathrm{rad/s}$ corresponding to $\dot{\varphi} = 0\,\mathrm{rad/s}$ and $\dot{\vartheta} = 1.7\,\mathrm{rad/s}$.

One can clearly see that the controller prioritizes the thrust alignment and thus the transient behavior divides into two

TABLE I

CONTROLLER AND PLANT PARAMETERS.

Controller parameters		
$\varphi_l = 10 \cdot \frac{\pi}{180}\,\text{rad}$	$v_{\varphi max} = 1.425\,\text{rad/s}$	$\Delta\varphi = \Delta\vartheta = 5 \cdot \frac{\pi}{180}\,\text{rad}$
$\vartheta_l = 15 \cdot \frac{\pi}{180}\,\text{rad}$	$v_{\vartheta max} = 0.624\,\text{rad/s}$	$\varphi_u = \vartheta_u = 175 \cdot \frac{\pi}{180}\,\text{rad}$
$c_\varphi = 0.817\,\text{Nm/rad}$	$\delta_\varphi = 0.1999\,\text{Nms/rad}$	$r_\varphi = r_\vartheta = 0.75$
$c_\vartheta = 0.109\,\text{Nm/rad}$	$\delta_z = 0.0961\,\text{Nms/rad}$	$v_\varphi = v_\vartheta = 0.1\,\text{rad/s}$
Plant parameters		
$\hat{\mathbf{J}} = \text{diag}(8.5, 8.5, 14) \cdot 10^{-3}\,\text{m}^2\text{kg}$		$\bar{\tau}_{xy} = 0.15\,\text{Nm}$
$\mathbf{J} = \hat{\mathbf{J}} + \Delta\mathbf{J}$		$\bar{\tau}_z = 0.03\,\text{Nm}$

phases. In the first phase lasting approximately 1.2 s the angle φ is made to zero meaning that the thrust vector is aligned. In a second phase $\varphi \approx 0$ is preserved, while the error angle ϑ is reduced to zero meaning that the desired orientation around the thrust axis is established.

As can be seen by the evolution of $\dot{\varphi}$, the first phase starts by accelerating the thrust vector until $\dot{\varphi}$ has approached the switching curve $s_\varphi(\varphi)$. Then, the behavior changes from acceleration to deceleration and in the region $\varphi \leq \varphi_l$ a soft transient to zero follows. During the whole process the control torque $\boldsymbol{\tau}_{xy}$ is exploited very well or even saturates at $\|\boldsymbol{\tau}_{xy}\| = \bar{\tau}_{xy}$.

Since the torque available in the z-direction is much smaller than the one in the xy-plane, the reduction of ϑ takes considerably longer, than the decrease of φ. At the beginning the initial angular velocity $\boldsymbol{\omega}_{z0} = 1.7^{\text{rad}}/\text{s}$ even leads to an increase of ϑ although the maximum available torque $\bar{\tau}_z$ is used to counteract the motion. Note that the saturation of τ_z in this first phase is mainly due to the damping, since the torque T_z stemming from the potential is small for large φ. After φ has decreased to zero, finally the reduction of ϑ begins. Again, a phase of acceleration is kept up until the switching curve $s_\vartheta(\vartheta)$ is approached and the deceleration is initiated. A soft transient to zero follows in the region $\vartheta \leq \vartheta_l$. In the nominal case the desired attitude is eventually reached after approximately 2 s. For all remaining simulations it takes no longer than approximately 2.5 s.

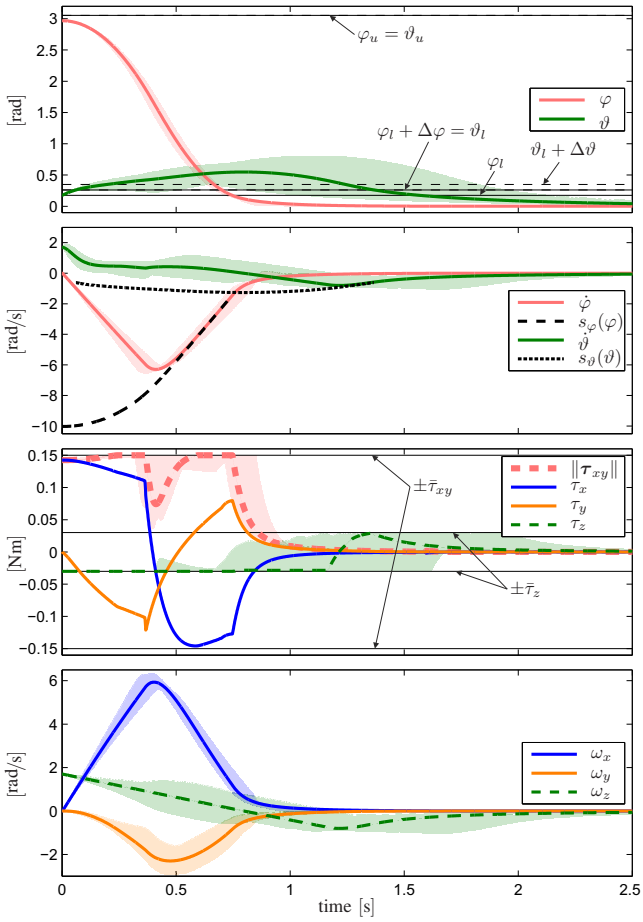

Fig. 3. Simulation results. Lines: Nominal closed loop. Shaded Areas: Closed loops with $\mathbf{J} = \hat{\mathbf{J}} + \Delta\mathbf{J}$.

VII. CONCLUSION

In this paper we have presented a fast and saturating attitude controller for a quadrotor helicopter. The nonlinear controller is based on an energy shaping approach and considers asymmetric control torque constraints. Almost global asymptotic stability of the desired attitude has been shown for arbitrary unknown moment of inertia matrices. The performance of the controller has been illustrated by simulations, which also have shown that the available control torques are exploited to a great extent or even saturated. The proposed controller prioritizes the alignment of the thrust and leads to a more or less sequential completion of the attitude control task.

REFERENCES

[1] S. P. Bhat and D. S. Bernstein, "A topological obstruction to continuous global stabilization of rotational motion and the unwinding phenomenon," *Systems & Control Letters*, vol. 39, no. 1, pp. 63–70, Jan. 2000.

[2] N. A. Chaturvedi, A. K. Sanyal, and N. H. McClamroch, "Rigid body attitude control," *IEEE Control Syst. Mag.*, vol. 31, pp. 30 – 51, June 2011.

[3] N. Chaturvedi and N. McClamroch, "Global stabilization of an inverted 3d pendulum including control saturation effects," in *Proc. Conference on Decision and Control*, 2006, pp. 6488–6493.

[4] O. Fritsch, P. De Monte, M. Buhl, and B. Lohmann, "Quasi-static feedback linearization for the translational dynamics of a quadrotor helicopter," in *Proc. American Control Conference*, 2012.

[5] O. Fritsch, B. Henze, and B. Lohmann, "Fast and saturating thrust direction control for a quadrotor helicopter," *at - Automatisierungstechnik*, vol. 61, no. 3, pp. 172–182, March 2013.

[6] J. F. Guerrero-Castellanos, N. Marchand, S. Lesecq, and J. Delamare, "Bounded attitude stabilization: Real-time application on four-rotor mini-helicopter," in *Proc. IFAC World Congress*, 2008.

[7] M.-D. Hua, T. Hamel, P. Morin, and C. Samson, "A control approach for thrust-propelled underactuated vehicles and its application to VTOL drones," *IEEE Trans. Automat. Contr.*, vol. 54, no. 8, pp. 1837–1853, Aug. 2009.

[8] N. Kottenstette and J. Porter, "Digital passive attitude and altitude control schemes for quadrotor aircraft," in *Proc. International Conference on Control and Automation (ICCA)*, dec. 2009, pp. 1761 –1768.

[9] M. Krstic, J. W. Modestino, and H. Deng, *Stabilization of Nonlinear Uncertain Systems*. New York: Springer, 1998.

[10] R. Ortega, A. V. D. Schaft, I. Mareels, and B. Maschke, "Putting energy back in control," *IEEE Control Syst. Mag.*, vol. 21, no. 2, pp. 18–33, 2001.

[11] M. Shuster, "A survey of attitude representations," *The Journal of the Astronautical Sciences*, vol. 41, no. 4, pp. 439–517, 1993.